

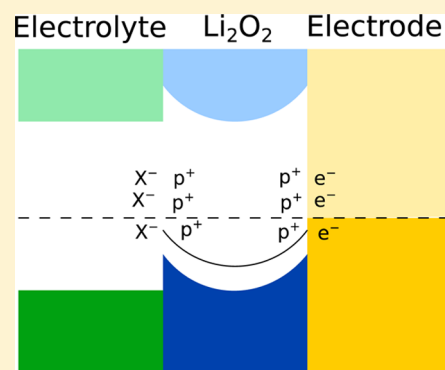
## Impact of Space-Charge Layers on Sudden Death in Li/O<sub>2</sub> Batteries

Maxwell D. Radin,<sup>†</sup> Charles W. Monroe,<sup>‡</sup> and Donald J. Siegel<sup>\*,§</sup>

<sup>†</sup>Department of Physics, <sup>‡</sup>Department of Chemical Engineering, and <sup>§</sup>Department of Mechanical Engineering, University of Michigan, 2350 Hayward Street, Ann Arbor, Michigan 48109, United States

**S** Supporting Information

**ABSTRACT:** The performance of Li/O<sub>2</sub> batteries is thought to be limited by charge transport through the solid Li<sub>2</sub>O<sub>2</sub> discharge product. Prior studies suggest that electron tunneling is the main transport mechanism through thin, compact Li<sub>2</sub>O<sub>2</sub> deposits. The present study employs a new continuum transport model to explore an alternative scenario, in which charge transport is mediated by polaron hopping. Unlike earlier models, which assume a uniform carrier concentration or local electroneutrality, the possibility of nonuniform space charge is accounted for at the Li<sub>2</sub>O<sub>2</sub>/electrolyte and Li<sub>2</sub>O<sub>2</sub>/electrode interfaces, providing a more realistic picture of transport in Li<sub>2</sub>O<sub>2</sub> films. The temperature and current-density dependences of the discharge curves predicted by the model are in good agreement with flat-electrode experiments over a wide range of rates, supporting the hypothesis that polaron hopping contributes significantly to charge transport. Exercising the model suggests that this mechanism could explain the observed enhancement in cell performance at elevated temperature and that performance could be further improved by tuning the interfacial orientation of Li<sub>2</sub>O<sub>2</sub> crystallites.



Charge transport through the solid Li<sub>2</sub>O<sub>2</sub> discharge product is expected to limit the performance of Li/O<sub>2</sub> batteries under some circumstances.<sup>1–4</sup> Previous computational<sup>3</sup> and experimental<sup>5,6</sup> studies have found that bulk Li<sub>2</sub>O<sub>2</sub> is a poor conductor; nevertheless, the nanometer-scale deposits frequently observed<sup>1,7,8</sup> in Li/O<sub>2</sub> cells may not exhibit the same behavior as bulk material. Several discharge mechanisms have been proposed, and the relative predominance of these mechanisms is expected to vary with cell design (e.g., choice of electrode material and electrolyte) and experimental conditions (e.g., temperature and discharge rate).<sup>2,9–11</sup> Some studies have reported that Li<sub>2</sub>O<sub>2</sub> can be electrodeposited in some cases as a thin, compact film, especially at the discharge rates relevant to automotive applications.<sup>1,8,12</sup> It has been proposed that charge transport through such films can limit cell performance during discharge.<sup>1,2</sup> Two mechanisms for charge transport in Li<sub>2</sub>O<sub>2</sub> films have been hypothesized: electron tunneling and the hopping of hole polarons.<sup>1–3,5,13</sup> Understanding the contributions from these two mechanisms—and how they vary with temperature, current density, film thickness, and orientation—has significance for battery engineering: the ability to enhance charge transport by optimizing cell design and operating parameters could allow for the improvement of battery performance.

Luntz et al.<sup>2</sup> presented a model for charge transport through Li<sub>2</sub>O<sub>2</sub> films in Li/O<sub>2</sub> cells that included both hole-polaron hopping and electron tunneling. They found that polaron transport could not explain the observed “sudden death” (i.e., the precipitous drop in cell potential that coincides with the end of discharge<sup>1,2</sup>) and that electron tunneling was the primary transport mechanism at practical current densities.

This model assumed that the concentration of polarons was uniform throughout the film, however. The present study extends the transport model of Luntz et al. by explicitly accounting for the spatial distribution of polarons.

Electroneutrality violations may play a role in transport phenomena if the thickness of a Li<sub>2</sub>O<sub>2</sub> deposit is smaller than the screening length associated with mobile charge carriers within it.<sup>2</sup> Prior density functional theory (DFT) calculations suggest that the intrinsic Fermi level of Li<sub>2</sub>O<sub>2</sub> is higher than both the Fermi levels of common electrode materials (e.g., carbon, gold, platinum) and the energy level associated with the redox potential of the Li<sup>+</sup>/O<sub>2</sub> couple (as shown in the Supporting Information (SI), Figure S1).<sup>1,14</sup> This suggests that space-charge layers containing high polaron concentrations may form in the discharge product near the Li<sub>2</sub>O<sub>2</sub>/electrode and Li<sub>2</sub>O<sub>2</sub>/electrolyte interfaces.

Some factors that drive charge accumulation at the interface between Li<sub>2</sub>O<sub>2</sub> and an electrode are illustrated schematically in Figure 1. In the absence of a space-charge layer, the intrinsic Fermi level of Li<sub>2</sub>O<sub>2</sub> is expected to be above that of the electrode; DFT calculations (Figure S1 in the SI) predict that the intrinsic Fermi level of Li<sub>2</sub>O<sub>2</sub> will be ~1.5 eV above the Fermi level of Au if the Li<sub>2</sub>O<sub>2</sub> film is terminated by the dominant surface facets, {11̄00} and {0001}.<sup>15</sup> Thus, when Li<sub>2</sub>O<sub>2</sub> and the electrode are placed in contact, a thermodynamic driving force induces electron transfer from the Li<sub>2</sub>O<sub>2</sub> to the

Received: May 16, 2015

Accepted: July 14, 2015

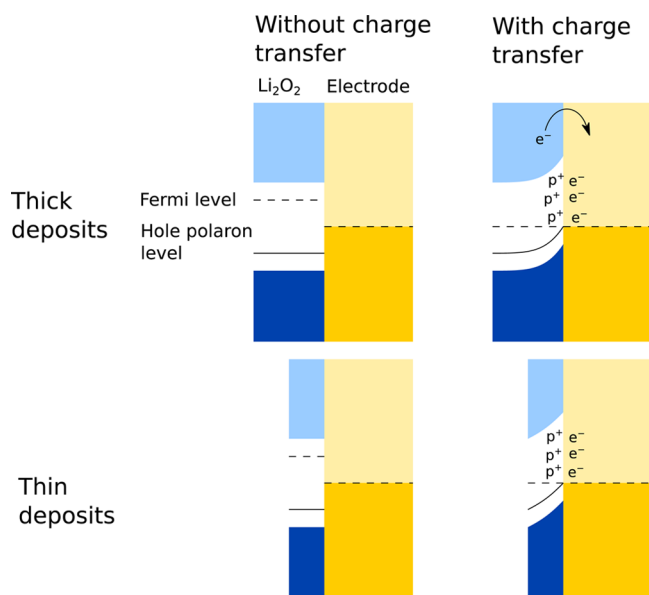
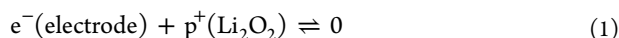
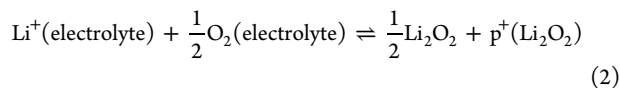


**Figure 1.** Schematic of double-layer formation at the  $\text{Li}_2\text{O}_2$ /electrode interface. Dark regions represent occupied electronic states, and light regions represent unoccupied states. The hole polarons and electrons accumulated within the space-charge layers are represented by  $\text{p}^+$  and  $\text{e}^-$ , respectively. When the  $\text{Li}_2\text{O}_2$  film thickness is smaller than the screening length associated with polarons (bottom right), enhanced polaron concentrations span the entire thickness of the film and consequently facilitate charge transport. When the film thickness is larger than the screening length (top right), the scarcity of polarons in the (central) bulk region limits charge transport.

electrode. This transfer creates hole polarons in  $\text{Li}_2\text{O}_2$ <sup>3,5</sup> through the annihilation reaction



Hole polarons have been identified as the dominant (positive) electronic charge carrier in  $\text{Li}_2\text{O}_2$ .<sup>3,5</sup> A double layer with a negative charge on the electrode surface and positive charge within the  $\text{Li}_2\text{O}_2$  results. At the  $\text{Li}_2\text{O}_2$ /electrolyte interface, an analogous process creates a thermodynamic driving force that pushes electrons out of  $\text{Li}_2\text{O}_2$  and drives the electrochemical half reaction



In this case, a similar double layer forms, with a positive space charge on  $\text{Li}_2\text{O}_2$  due to hole polarons and a negative space charge in the electrolyte arising from a paucity of  $\text{Li}^+$ . In short, the calculated alignment of energy levels suggests that hole polarons should accumulate within  $\text{Li}_2\text{O}_2$  near its interfaces with both the electrode and the electrolyte.

A 1-D transport model based on nonelectroneutral Nernst–Planck theory was developed to explore how enhanced polaron concentration within space-charge layers could affect the performance of a  $\text{Li}/\text{O}_2$  cell. The model allows for the quantification of hole-polaron transport rates through thin  $\text{Li}_2\text{O}_2$  films and can reproduce discharge curves from flat-electrode experiments. Importantly, the model shows that space-charge effects can explain sudden death behavior which occurs when the thickness of the growing film exceeds the characteristic thickness of the space-charge layer, as shown in Figure 1. As films thicken, charge transport becomes limited by

the low concentration of polarons in the bulk, resulting in sudden death.

The model assumes that transport within the film is quasi-steady, meaning that diffusional relaxations associated with the local accumulation of polarons occur very rapidly in comparison with the time scale of interest; it also assumes that the film thickness changes sufficiently slowly that the velocity of the  $\text{Li}_2\text{O}_2$ /electrolyte boundary can be neglected. These assumptions are supported by the fact that the characteristic diffusion length  $\sqrt{Dt}$  (where  $D$  is the polaron diffusion coefficient and  $t$  is the discharge duration) is much larger than the film thickness within the parameter space of primary interest.

The conceptual basis of the model is illustrated in Figure 2. The  $\text{Li}_2\text{O}_2$  is taken to be a planar, isotropic film; the position

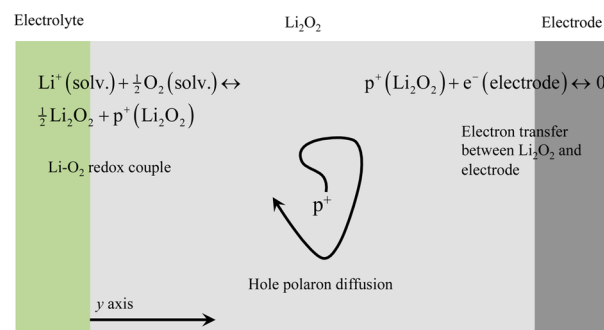


**Figure 2.** Schematic of transport model.

variable  $y$  quantifies the distance into the  $\text{Li}_2\text{O}_2$  film, with the film/electrolyte and film/electrode interfaces being located at  $y = 0$  and  $y = L$ , respectively. Maxwell's equations imply that charge density satisfies a continuity equation. In a quasi-steady state, charge continuity requires that the current density  $i$  is divergence-free throughout the film:  $di/dy = 0$ . The potential distribution within the  $\text{Li}_2\text{O}_2$  also satisfies Poisson's equation

$$\frac{d^2\Phi}{dy^2} = -\frac{\rho}{\epsilon} \quad (3)$$

where  $\epsilon$  is the dielectric permittivity of the film and  $\rho(y)$  is the excess charge density.

The diffusion and migration of hole polarons is modeled by a Nernst–Planck flux law

$$N = -\frac{DF}{RT}c \frac{d\Phi}{dy} - D \frac{dc}{dy} \quad (4)$$

where  $c$  is the molar polaron concentration,  $D$  is the polaron diffusivity,  $F$  is Faraday's constant, and  $RT$  is the molar thermal energy. The molar flux of polarons,  $N$ , relates to the charge flux through Faraday's law,  $i = FN$ ; the polaron concentration relates to the excess charge density through  $\rho = cF$ .

At the film/electrode interface, charge transfer between the  $\text{Li}_2\text{O}_2$  and electrode support occurs through annihilation reaction 1. The chemical potential of polarons at the film boundary is taken to balance that of electrons in the support, causing the polaron concentration to satisfy a mass-action law  $c(L) = c_L$ . At the film/electrolyte interface, the  $\text{Li}/\text{O}_2$  redox reaction proceeds through half-reaction 2, in which polarons have a different chemical potential than in reaction 1 because of free-energy losses due to charge transport through the film. The electrochemical potentials of polarons and peroxide in the film

balance those of lithium and oxygen in the adjacent electrolyte, however, yielding a mass-action law that fixes the polaron concentration at the film/electrolyte interface,  $c(0) = c_0$ .

The previous paragraphs contain a complete mathematical statement of the model, which can be simplified by introducing a dimensionless position  $\xi = y/L$  and dimensionless concentration  $\Theta(\xi) = 2c(y)/(c_0 + c_L)$ . Through combination of the equations governing material and charge continuity with Poisson's equation, this dimensionless concentration can be shown to satisfy the single ordinary governing equation

$$0 = \frac{d^2\Theta}{d\xi^2} - \beta^2\Theta^2 - j\frac{1}{\Theta}\frac{d\Theta}{d\xi} - \frac{1}{\Theta}\left(\frac{d\Theta}{d\xi}\right)^2 \quad (5)$$

Here  $j = 2iL/FD(c_0 + c_L)$  represents a dimensionless current density and  $\beta = [F^2L^2(c_0 + c_L)/2\varepsilon RT]^{1/2}$  is a dimensionless film thickness (i.e., a film thickness in units of the screening length associated with polaron concentration  $(c_0 + c_L)/2$ ). The dimensionless concentration  $\Theta$  satisfies boundary conditions  $\Theta(0) = 2/(1 + s)$  and  $\Theta(1) = 2s/(1 + s)$ , where  $s = c_L/c_0$ . The dimensionless voltage drop  $\Delta\phi = F[\Phi(L) - \Phi(0)]/RT$  can be expressed as

$$\Delta\phi = -\int_0^1 \frac{j}{\Theta} d\xi - \log s \quad (6)$$

and the overpotential  $\eta_{\text{passivation}}$  arising from charge-transport limitations within the  $\text{Li}_2\text{O}_2$  film is given by

$$\eta_{\text{passivation}} = \frac{RT}{F}(\Delta\phi - \log s) \quad (7)$$

Note that the model is invariant under reflection symmetry (in the sense that  $j \rightarrow -j$  and  $\xi \rightarrow 1 - \xi$  implies  $\eta(-j) = -\eta(j)$ ) when  $s = 1$ . Otherwise the overpotentials associated with discharge and recharge may be asymmetric.

Analytic solutions to the model can be obtained in certain limits. If the dimensionless film thickness is large ( $\beta \gg 1$ ), then eq 5 can be transformed with  $\Theta = \Theta'/\beta^2$  to yield

$$0 = \frac{d^2\Theta'}{d\xi^2} - \Theta'^2 - j\beta^2\frac{1}{\Theta'}\frac{d\Theta'}{d\xi} - \frac{1}{\Theta'}\left(\frac{d\Theta'}{d\xi}\right)^2 \quad (8)$$

where  $\Theta'$  satisfies the boundary conditions  $\Theta'(0) = \Theta'(1) = \infty$ . In the regime where current is sufficiently small that  $j\beta^2 \ll 1$ , the solution is

$$\Theta' = \frac{4\pi^2}{1 + \cos\left[2\pi\left(\xi - \frac{1}{2}\right)\right]} \quad (9)$$

This yields  $\Delta\phi - (\Delta\phi)_{j=0} = -j\beta^2/4\pi^2$ , and an overpotential of

$$\eta_{\text{passivation}} = -\frac{1}{4\pi^2} \frac{iL^3}{D\varepsilon} \quad (10)$$

Equation 10 demonstrates a few important points regarding the overpotential in the thick-film/small-current limit:

(1) The overpotential is independent of the boundary concentrations  $c_0$  and  $c_L$ ; consequently discharge and recharge are symmetric,  $\eta(-j) = -\eta(j)$ , even if  $s \neq 1$ .

(2) The overpotential increases with the cube of the film thickness, consistent with sudden death behavior.

(3) The temperature dependence of overpotential is determined by the product  $D\varepsilon$ . For thermally activated polaron hopping,  $D$  increases exponentially with temperature. In

contrast,  $\varepsilon$  will have little dependence on temperature for a nonpolar material like  $\text{Li}_2\text{O}_2$ . Thus, the overpotential should decrease with increasing temperature.

A second scenario of interest is the thin-film limit,  $\beta \rightarrow 0$ , where one can neglect the  $\beta^2\Theta^2$  term in eq 5 and obtain the current density as a function of voltage,

$$j = -\frac{se^{\Delta\phi} - 1}{e^{\Delta\phi} - 1}\Delta\phi \quad (11)$$

In this limit, the overpotential associated with charge-transport limitations,  $\eta_{\text{passivation}}$ , becomes Ohmic (i.e., proportional to film thickness and current) if the current is large or small:

$$-\frac{F^2D\eta}{iLRT} = \begin{cases} 1/c_L & \text{when } j \ll -1 \\ (1/c_0 - 1/c_L)/\ln(c_0/c_L) & \text{when } |j| \ll 1 \\ 1/c_0 & \text{when } j \gg 1 \end{cases} \quad (12)$$

Unlike the thick-film/low-current regime, the overpotential in the thin-film limit is asymmetric when the polaron concentrations at the  $\text{Li}_2\text{O}_2$ /electrode and  $\text{Li}_2\text{O}_2$ /electrolyte interfaces differ ( $s \neq 1$ ). The thin-film/high-current regime can be understood simply: The polaron concentration throughout most of the film matches the concentration at the interface where the current flows out, except for an infinitesimally small region near the opposite boundary.

To make comparisons to experimental data that relate discharge potential to capacity (or equivalently, to film thickness), it is necessary to include the contribution of the kinetics of the  $\text{Li}/\text{O}_2$  couple to the cell potential  $E$ . The cell potential can generally be expressed in the form

$$E = E^0 + \eta_{\text{kinetic}} + \eta_{\text{passivation}} \quad (13)$$

where  $E^0$  is the equilibrium cell potential (2.96 V vs  $\text{Li}/\text{Li}^+$  at a temperature of 298.15 K<sup>16</sup>),  $\eta_{\text{passivation}}$  is given by eq 7, and  $\eta_{\text{kinetic}}$  is determined by the Butler–Volmer equation

$$i = i_0 \left\{ \exp\left(-\frac{\alpha F\eta_{\text{kinetic}}}{RT}\right) - \exp\left[\frac{(1-\alpha)F\eta_{\text{kinetic}}}{RT}\right] \right\} \quad (14)$$

For simplicity, the symmetry factor  $\alpha$  is taken to be 1/2, and overpotential is assumed to be negative and in the Tafel regime (large in magnitude relative to  $RT/F$ ). The kinetic overpotential can then be approximated as

$$\eta_{\text{kinetic}} = -2\frac{RT}{F} \ln \frac{i}{i_0} \quad (15)$$

The left panel of Figure 3 shows the potential calculated from eq 13 as a function of cell capacity and film thickness for current densities spanning three orders of magnitude. The passivation overpotential  $\eta_{\text{passivation}}$  was determined from eqs 6 and 7, using the dimensionless polaron concentration  $\Theta$  obtained from the numerical solution of eq 5. Here the density of  $\text{Li}_2\text{O}_2$ <sup>17</sup> has been used to relate the capacity to film thickness; a capacity of 1  $\mu\text{Ah}/\text{cm}^2$  corresponds to a thickness of 3.7 nm. The values for the polaron diffusivity,  $D$ , dielectric permittivity,  $\varepsilon$ , and exchange-current density,  $i_0$ , were informed by prior calculations and experiments<sup>3,18,19</sup> and subsequently adjusted to match discharge curves from flat-electrode experiments,<sup>2</sup> which are reproduced in the right panel of Figure 3. These experiments were designed to probe charge transport through

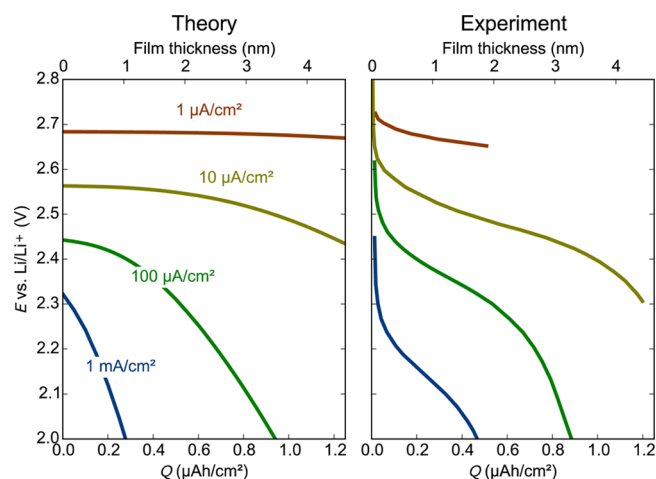


**Figure 3.** Potential as a function of discharge capacity and film thickness for uniform  $\text{Li}_2\text{O}_2$  deposition predicted by the model (left) and as measured by flat-electrode experiments (right). Experimental data adapted from Luntz et al.<sup>2</sup>

thin  $\text{Li}_2\text{O}_2$  films and removed some of the complications of a “practical”  $\text{Li}/\text{O}_2$  cell through the use of a flat electrode and stirred electrolyte.<sup>2,20</sup> Although no experimental or theoretical values for the boundary concentrations  $c_0$  and  $c_L$  have been reported, physically reasonable values were chosen: the boundary concentrations represent a small fraction (1%) of the concentration of possible polaron sites (i.e.,  $\text{O}_2$  dimers) in the  $\text{Li}_2\text{O}_2$  lattice. (The boundary concentrations were assumed to match,  $c_0 = c_L$  or  $s = 1$ , for simplicity.) All the model parameters are summarized alongside literature values in Table 1.

**Table 1. Parameter Values Used in the Model and Relevant Values from the Literature**

parameter	description	value used in model	other reported values
$D$	polaron diffusion coefficient	$3 \times 10^{-13} \text{ cm}^2/\text{s}$	$9 \times 10^{-10} \text{ cm}^2/\text{s}$ (in-plane) <sup>3</sup> $2 \times 10^{-14} \text{ cm}^2/\text{s}$ (out-of-plane) <sup>3</sup>
$\epsilon/\epsilon_0$	$\text{Li}_2\text{O}_2$ dielectric constant	10	$\epsilon_{xx}/\epsilon_0 = \epsilon_{yy}/\epsilon_0 = 7.5$ ; $\epsilon_{zz}/\epsilon_0 = 12.5$ <sup>3</sup>
$i_0$	exchange current density	$5 \times 10^{-9} \text{ A}/\text{cm}^2$	$10^{-5} \text{ A}/\text{cm}^2$ <sup>218</sup> $10^{-9} \text{ A}/\text{cm}^2$ <sup>219</sup>
$c_1 = c_2$	polaron concentration at interfaces	$3 \times 10^{20} \text{ cm}^{-3}$ (1% occupancy)	

The curves in Figure 3 illustrate the effect of electrical passivation on discharge voltage: the voltage decreases with increasing thickness, and the decrease becomes more severe at higher current densities. The model qualitatively reproduces the sudden death observed in the experiments: the magnitude of the charge-transport overpotential increases superlinearly with film thickness. This is expected from the thick-film/low-current expression from eq 10, which approximates the 1 and  $10 \mu\text{A}/\text{cm}^2$  cases. (The thick-film condition  $\beta \gg 1$  corresponds to  $L \gg 0.2 \text{ nm}$ , and for  $L = 1 \text{ nm}$  the low-current condition  $j\beta^2 \ll 1$  corresponds to  $i \ll 29 \mu\text{A}/\text{cm}^2$ .) At a current density of  $1 \text{ mA}/\text{cm}^2$ , the low-current condition is not satisfied, and so the shape of the discharge curve qualitatively changes: the potential

is highly sloped at the beginning of discharge rather than being flat.

This sudden-death behavior can be understood by examining polaron concentration profiles, shown for a current density of  $100 \mu\text{A}/\text{cm}^2$  in Figure 4 for  $\text{Li}_2\text{O}_2$  films of thicknesses ranging

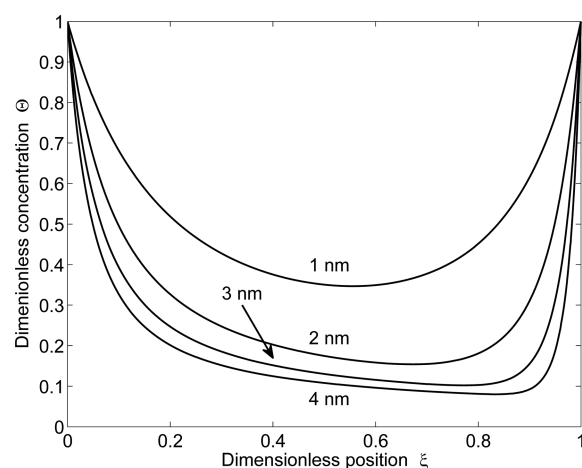


**Figure 4.** Dimensionless concentration of polarons within a  $\text{Li}_2\text{O}_2$  film at a discharge current of  $100 \mu\text{A}/\text{cm}^2$  for film thicknesses from 1 to 4 nm. The current flows to the right.

from 1 to 4 nm. Polarons accumulate at the  $\text{Li}_2\text{O}_2$ /electrolyte and  $\text{Li}_2\text{O}_2$ /electrode interfaces, consistent with the schematic in Figure 1. As the thickness increases, the concentration of polarons on the interior of the film decreases, and thus stronger electric fields are needed to maintain the same current across the film. Because the strength of the electric field must increase as the film thickness increases, the magnitude of the potential drop increases faster than linearly with film thickness. The asymmetry in the spatial distribution of polarons arises from the depletion of polarons near the  $\text{Li}_2\text{O}_2$ /electrode interface as they are consumed by reaction 1.

On the basis of the good qualitative and quantitative agreement between the discharge curves predicted by the model and those measured experimentally, we hypothesize that polaron diffusion, rather than electron tunneling, is the dominant charge-transport mechanism through thin films in  $\text{Li}/\text{O}_2$  cells. This contrasts with the conclusions of Luntz et al.,<sup>2</sup> who argued that hole-polaron-mediated transport could not explain the sudden-death behavior observed in discharge experiments. The reason for this discrepancy is that the model of Luntz et al. takes the polaron concentration to be uniform throughout the film, an assumption that the present model reveals to be valid only in the extreme thin-film limit. On the basis of the parameters in Table 1, typical experiments do not probe this limit because the thin-film condition  $\beta \ll 1$  corresponds to  $L \ll 0.2 \text{ nm}$ . Realistically, one should expect polaron concentrations to be highly nonuniform, which Figure 4 illustrates to be the case for any film thicker than a single monolayer of  $\text{Li}_2\text{O}_2$ . We conclude that accounting for the spatial variation of the polaron concentration is essential when estimating charge-transport rates within the discharge product of a  $\text{Li}/\text{O}_2$  cell. Also, we note that oxygen-transport limitations can cause a similar sudden-death behavior under some experimental conditions;<sup>21,22</sup> however, the experiments of Luntz et al. in principle removed liquid-phase transport limitations by vigorously stirring the electrolyte.<sup>2,20</sup>

The present model also correctly captures the impact of temperature on the Li/O<sub>2</sub> discharge curve observed in flat-electrode experiments. For example, in the thick-film/low-current regime described by eq 10, temperature dependence enters primarily through the polaron diffusivity, which scales with temperature as  $D \sim T \exp(-E/k_B T)$ . The fact that  $\eta_{\text{passivation}}$  is inversely proportional to  $D$  suggests that increasing the temperature will enhance discharge capacity, a trend borne out by the flat-electrode experiments of Luntz et al.<sup>2</sup> and by other experiments using porous electrodes.<sup>4,23</sup> (However, in experiments employing porous-electrode-based cells, other factors could also play a role in the temperature dependence; for example, because O<sub>2</sub> transport is uncontrolled in these cells, the sensitivity of O<sub>2</sub> solubility in the electrolyte to temperature could contribute to the temperature dependence of performance.) Furthermore, because  $\eta_{\text{passivation}}$  is proportional to the ratio of the current density to the diffusion coefficient  $i/D$ , the model suggests that the shape of the discharge curve will be unchanged if the temperature and current are increased in the similar proportions. This scaling behavior is evident in the experimental discharge curves shown by Luntz et al.<sup>2</sup> (Figure 2a and Figure S5a in the SI); for example, a cell discharged at 3  $\mu\text{A}$  at 20 °C yields a discharge curve nearly identical to a cell discharged at approximately twice the rate (5  $\mu\text{A}$ ) at the higher temperature of 40 °C. This comparison implies an activation energy for polaron hopping of  $\sim 0.2$  eV. DFT calculations previously estimated in-plane hole polaron hopping barriers of 0.42<sup>3</sup> and 0.39<sup>24</sup> eV in Li<sub>2</sub>O<sub>2</sub>. Considering the uncertainties in the calculations and experiments, this is reasonable agreement.

In contrast, Luntz et al. speculate that electron tunneling would not exhibit a significant temperature dependence over the relevant temperature range.<sup>2</sup> The increased discharge capacity observed at elevated temperatures in flat- and porous-electrode experiments, as previously discussed, lends additional support to the notion that hole-polaron diffusion contributes significantly to charge transport in Li/O<sub>2</sub> cells; still, one cannot exclude the possibility that the tunneling rate does vary significantly with temperature.

Another feature commonly observed in experiments, on both flat<sup>2</sup> and porous<sup>25</sup> electrodes, is a strong asymmetry between discharge and charge; that is, for a fixed current and nominal film thickness the magnitude of the overpotential differs between discharge and recharge. As previously discussed, the present model naturally produces an asymmetry when the polaron concentrations at the Li<sub>2</sub>O<sub>2</sub>/electrode and Li<sub>2</sub>O<sub>2</sub>/electrolyte interfaces differ.

It is worthwhile to touch upon the transient behavior seen in the first  $\sim 0.1 \mu\text{Ah}/\text{cm}^2$  of experimental discharge data shown in Figure 3. This feature is not reproduced by our model or previous models.<sup>2</sup> We speculate that it could arise from a capacitive relaxation, a macroscopic oxygen-diffusion transient, or side reactions on the exposed carbon electrode's surface (e.g., the formation of Li<sub>2</sub>CO<sub>3</sub>, as suggested in ref 18.).

There are two features in the experimental flat-electrode charging curves of Luntz et al. (shown in figures S3 and S4 in the supporting information of that work<sup>2</sup>) that cannot be reproduced by our model regardless of the choice of parameters. First, in experiments the overpotential is observed to rise as charging proceeds.<sup>2</sup> This behavior is absent in our model because as charging proceeds the film becomes thinner and overpotentials necessarily decrease in magnitude. Second, the experimentally observed overpotential is not uniquely determined by the capacity and current, as can be seen from

Figure S4 in the SI of that study. This implies that there is some other property that changes as recharge proceeds, such as composition or morphology. In fact, the overpotential appears to be uniquely determined by the *fractional* capacity and current.

The dramatic qualitative differences between experimental discharge and recharge curves suggest that the recharge mechanism differs fundamentally from the discharge mechanism. Several possibilities have been proposed:

- The accumulation of side-reaction products at the Li<sub>2</sub>O<sub>2</sub>/electrolyte interface during recharge could cause potential to rise as charging proceeds.<sup>18</sup>

- Discharge<sup>9,10</sup> or recharge<sup>26</sup> could be mediated by soluble species, such as superoxide radicals.

- Recharge could occur via the partial delithiation of the discharge product, via either a two-phase or solid-solution pathway.<sup>3,27–29</sup>

- Discharge may occur homogeneously, while recharge does not. In other words, perturbations to the smoothness of the film that are stable during discharge may be unstable during charge. Such a phenomenon could be caused by charge-transport limitations: dimples in the film may become amplified during recharge because charge transport is most facile in locations where the film is thinnest. Generalizing our model to three dimensions could capture such an effect.

Finally, the model suggests that crystallite orientation has implications for cell performance. Charge transport via hole polarons is sensitive to crystallographic orientation because there is substantial inherent anisotropy in the dielectric and polaron-diffusion tensors. Although anisotropy has been neglected in the present model, the fact that the in-plane polaron hopping barrier calculated with DFT is 0.1 to 0.3 eV<sup>3,24</sup> smaller than the out-of-plane barrier<sup>3</sup> indicates that transport overpotentials will be lower in films where the {0001} axis lies in the plane of electrode surface; thus we speculate that Li/O<sub>2</sub> cells designed to align crystallites in this orientation will exhibit superior discharge performance.

In summary, a model has been developed to illustrate how space-charge layers affect charge transport through thin Li<sub>2</sub>O<sub>2</sub> films in a Li/O<sub>2</sub> electrochemical cell. The model accounts both for electroneutrality violations and for the nonuniform distribution of charge carriers. Sudden-death behavior during discharge is shown to be consistent with polaron-hopping limitations, contrary to the conclusions of prior studies. Such sudden death occurs when the film grows thick enough that the space-charge layer can no longer provide a sufficient concentration of polarons in the interior of the film to satisfy current-density requirements. The good agreement between the predicted overpotentials and experimental data as a function of current, film thickness, and temperature suggests that hole-polaron diffusion within space-charge layers is the dominant charge-transport mechanism in thin, compact Li<sub>2</sub>O<sub>2</sub> deposits during discharge. This challenges the previously proposed notion that electron tunneling dominates. The existence of space-charge-mediated polaron transport indicates that discharge performance can be improved by increasing the operating temperature or by orienting Li<sub>2</sub>O<sub>2</sub> crystallites to align the {0001} crystal axis normal to the electrode surface.

**■ ASSOCIATED CONTENT****■ Supporting Information**

Alignment of energy levels in a Li/O<sub>2</sub> cell. The Supporting Information is available free of charge on the ACS Publications website at DOI: 10.1021/acs.jpcllett.5b01015.

**■ AUTHOR INFORMATION****Corresponding Author**

\*E-mail: djsiege@umich.edu.

**Notes**

The authors declare no competing financial interest.

**■ ACKNOWLEDGMENTS**

This work was supported by the U.S. National Science Foundation through grant nos. CBET-1351482 and CBET-1336387

**■ REFERENCES**

- (1) Viswanathan, V.; Thygesen, K. S.; Hummelshøj, J. S.; Nørskov, J. K.; Girishkumar, G.; McCloskey, B. D.; Luntz, A. C. Electrical Conductivity in Li<sub>2</sub>O<sub>2</sub> and Its Role in Determining Capacity Limitations in Non-Aqueous Li-O<sub>2</sub> Batteries. *J. Chem. Phys.* **2011**, *135*, 214704.
- (2) Luntz, A. C.; Viswanathan, V.; Voss, J.; Varley, J. B.; Speidel, A. Tunneling and Polaron Charge Transport through Li<sub>2</sub>O<sub>2</sub> in Li-O<sub>2</sub> Batteries. *J. Phys. Chem. Lett.* **2013**, *4*, 3494–3499.
- (3) Radin, M. D.; Siegel, D. J. Charge Transport in Lithium Peroxide: Relevance for Rechargeable Metal-Air Batteries. *Energy Environ. Sci.* **2013**, *6*, 2370–2379.
- (4) Das, S. K.; Xu, S.; Emwas, A.-H.; Lu, Y. Y.; Srivastava, S.; Archer, L. a. High Energy Lithium-Oxygen Batteries - Transport Barriers and Thermodynamics. *Energy Environ. Sci.* **2012**, *5*, 8927.
- (5) Gerbig, O.; Merkle, R.; Maier, J. Electron and Ion Transport In Li<sub>2</sub>O<sub>2</sub>. *Adv. Mater.* **2013**, *25*, 3129–3133.
- (6) Dunst, a.; Epp, V.; Hanzu, I.; Freunberger, S. a.; Wilkening, M. Short-Range Li Diffusion vs. Long-Range Ionic Conduction in Nanocrystalline Lithium Peroxide Li<sub>2</sub>O<sub>2</sub>—the Discharge Product in Lithium-Air Batteries. *Energy Environ. Sci.* **2014**, *7*, 2739–2752.
- (7) Horstmann, B.; Gallant, B.; Mitchell, R.; Bessler, W. G.; Shao-horn, Y.; Bazant, M. Z. Rate-Dependent Morphology of Li<sub>2</sub>O<sub>2</sub> Growth in Li-O<sub>2</sub> Batteries. *J. Phys. Chem. Lett.* **2013**, *4*, 4217–4222.
- (8) Adams, B. D.; Radtke, C.; Black, R.; Trudeau, M. L.; Zaghbi, K.; Nazar, L. F. Current Density Dependence of Peroxide Formation in the Li-O<sub>2</sub> Battery and Its Effect on Charge. *Energy Environ. Sci.* **2013**, *6*, 1772.
- (9) Safari, M.; Adams, B. D.; Nazar, L. F. Kinetics of Oxygen Reduction in Aprotic Li-O<sub>2</sub> Cells: A Model-Based Study. *J. Phys. Chem. Lett.* **2014**, *5*, 3486–3491.
- (10) Xue, K.; Mcturk, E.; Johnson, L.; Bruce, P. G.; Franco, A. A. A Comprehensive Model for Non-Aqueous Lithium Air Batteries Involving Different Reaction Mechanisms. *J. Electrochem. Soc.* **2015**, *162*, 614–621.
- (11) Aetukuri, N. B.; McCloskey, B. D.; García, J. M.; Krupp, L. E.; Viswanathan, V.; Luntz, A. C. Solvating Additives Drive Solution-Mediated Electrochemistry and Enhance Toroid Growth in Non-Aqueous Li-O<sub>2</sub> Batteries. *Nat. Chem.* **2014**, *7*, 50–56.
- (12) Wen, R.; Hong, M.; Byon, H. R. In Situ AFM Imaging of Li-O<sub>2</sub> Electrochemical Reaction on Highly Oriented Pyrolytic Graphite with Ether-Based Electrolyte. *J. Am. Chem. Soc.* **2013**, *135*, 10870–10876.
- (13) Ong, S. P.; Mo, Y.; Ceder, G. Low Hole Polaron Migration Barrier in Lithium Peroxide. *Phys. Rev. B: Condens. Matter Mater. Phys.* **2012**, *85*, 081105.
- (14) Varley, J. B.; Viswanathan, V.; Nørskov, J. K.; Luntz, A. C. Lithium and Oxygen Vacancies and Their Role in Li<sub>2</sub>O<sub>2</sub> Charge Transport in Li-O<sub>2</sub> Batteries. *Energy Environ. Sci.* **2014**, *7*, 720–727.
- (15) Radin, M. D. *First-Principles and Continuum Modeling of Charge Transport in Li-O<sub>2</sub> Batteries*; University of Michigan: Ann Arbor, MI, 2014.
- (16) Chase, M. W., Jr. *NIST-JANAF Thermochemical Tables*; Chase, M. W., Ed.; American Chemical Society: Washington, DC, 1998.
- (17) *CRC Handbook of Chemistry and Physics*, 93rd ed.; Haynes, W. M., Ed.; CRC Press: Cleveland, OH, 2013.
- (18) McCloskey, B. D.; Speidel, A.; Scheffler, R.; Miller, D. C.; Viswanathan, V.; Hummelshøj, J. S.; Nørskov, J. K.; Luntz, A. C. Twin Problems of Interfacial Carbonate Formation in Nonaqueous Li-O<sub>2</sub> Batteries. *J. Phys. Chem. Lett.* **2012**, *3*, 997–1001.
- (19) Imanishi, N.; Luntz, A. C.; Bruce, P. *The Lithium Air Battery: Fundamentals*; Imanishi, N., Bruce, P., Luntz, A. C., Eds.; Springer: New York, 2014.
- (20) McCloskey, B.; Scheffler, R.; Speidel, A.; Girishkumar, G.; Luntz, A. C. On the Mechanism of Non-Aqueous Li-O<sub>2</sub> Electrochemistry on C and Its Kinetic Overpotentials: Some Implications for Li-Air Batteries. *J. Phys. Chem. C* **2012**, *116*, 23897–23905.
- (21) Griffith, L. D.; Sleightholme, A.; Mansfield, J. F.; Siegel, D. J.; Monroe, C. W. Correlating Li/O<sub>2</sub> Cell Capacity and Product Morphology with Discharge Current. *ACS Appl. Mater. Interfaces* **2015**, *7*, 7670.
- (22) Chen, X. J.; Bevara, V. V.; Andrei, P.; Hendrickson, M.; Plichta, E. J.; Zheng, J. P. Combined Effects of Oxygen Diffusion and Electronic Resistance in Li-Air Batteries with Carbon Nanofiber Cathodes. *J. Electrochem. Soc.* **2014**, *161*, A1877–A1883.
- (23) Song, M.; Zhu, D.; Zhang, L.; Wang, X.; Mi, R.; Liu, H.; Mei, J.; Lau, L. W. M.; Chen, Y. Temperature Characteristics of Nonaqueous Li-O<sub>2</sub> Batteries. *J. Solid State Electrochem.* **2014**, *18*, 739–745.
- (24) García-Lastra, J. M.; Myrdal, J. S. G.; Christensen, R.; Thygesen, K. S.; Vegge, T. DFT+U Study of Polaronic Conduction in Li<sub>2</sub>O<sub>2</sub> and Li<sub>2</sub>CO<sub>3</sub>: Implications for Li-Air Batteries. *J. Phys. Chem. C* **2013**, *117*, 5568.
- (25) McCloskey, B.; Bethune, D.; Shelby, R.; Girishkumar, G.; Luntz, A. Solvents' Critical Role in Nonaqueous Lithium-Oxygen Battery. *J. Phys. Chem. Lett.* **2011**, *2*, 1161–1166.
- (26) Meini, S.; Solchenbach, S.; Piana, M.; Gasteiger, H. a. The Role of Electrolyte Solvent Stability and Electrolyte Impurities in the Electrooxidation of Li<sub>2</sub>O<sub>2</sub> in Li-O<sub>2</sub> Batteries. *J. Electrochem. Soc.* **2014**, *161*, A1306–A1314.
- (27) Kang, S.; Mo, Y.; Ong, S. P.; Ceder, G. A Facile Mechanism for Recharging Li<sub>2</sub>O<sub>2</sub> in Li-O<sub>2</sub> Batteries. *Chem. Mater.* **2013**, *25*, 3328–3336.
- (28) Gallant, B. M.; Kwabi, D. G.; Mitchell, R. R.; Zhou, J.; Thompson, C. V.; Shao-Horn, Y. Influence of Li<sub>2</sub>O<sub>2</sub> Morphology on Oxygen Reduction and Evolution Kinetics in Li-O<sub>2</sub> Batteries. *Energy Environ. Sci.* **2013**, *6*, 2518.
- (29) Radin, M. D.; Monroe, C. W.; Siegel, D. J. How Dopants Can Enhance Charge Transport in Li<sub>2</sub>O<sub>2</sub>. *Chem. Mater.* **2015**, *27*, 839–847.